Broadband Conformal frequency independent Antenna for Airborne Applications

Ravi Kumar Agrahari*(1), Kundan Kumar Suman (1), Rahul Singh (1), and Ravi Kumar Gangwar (1)
(1)Department of Electronics Engineering, Indian Institute of Technology (Indian School of Mines), Dhanbad, India
(1)* raviagrahari652@gmail.com

1. Introduction

Broadband antennas are currently very appealing for airborne [1] applications. However, due to the requirements for conformality, flexibility, and robustness, antenna design for such applications is difficult. Conformal antennas that can be mounted on any arbitrary curved surface have garnered increased attention in recent years. The utility of these antennas for a missile or unmanned aerial vehicle is one of the most influential aspects of their significance. The primary goal of creating conformal antenna structures is to achieve omnidirectional azimuthal coverage. The antenna must typically be low profile and flexible in order to achieve a perfect attachment to a given surface. As a result, printed antennas have become the most commonly used form in the design of microwave conformal antennas [2,3]. Spirals and helices are used in the literature to achieve broadband characteristics with circular polarization. Indeed, spiral antenna designs, on the other hand, are easily realized using PCB technology and readily conformable.

Spiral antennas are circularly polarized (CP) antennas with relatively constant input impedance and radiation pattern characteristics over a broad frequency band. They are utilized in numerous communication platforms, navigational systems, and ground and space exploration stations [4–6]. Due to their wide impedance bandwidth, spiral antennas are considered frequency-independent (FI) antennas. The effective aperture of the ideal FI antenna for low-frequency radiations must be infinitely large. To overcome the high-frequency limitations, the feed region must be infinitesimally small and microscopic [7]. Only a FI antenna has distinct near-field and far-field characteristics in this situation. Typically, the upper frequency limit is determined by the balance-to-unbalance (balun) accuracy and the size of the excitation network.

In this paper, we suggest a BSA, which is fed by a balun to excite the balanced mode. The antenna that was designed has been built, and its performance has been measured. Here's how the rest of this paper is put together; The Archimedean spiral antenna and Balun design is talked about in Section 2. In Section 3, the parametric studies of simulated near-field and far-field characteristics of conformal BSA have been discussed. In section 4, the experimental validation is given and the last part of this paper is the conclusion, which is in Section 5.

2. Conformal Spiral Antenna with Balun

2.1 Spiral antenna design

An antenna consisting of a self-complementary Archimedean spiral with two non-planar arms is designed. The spiral antenna is designed on FR4 substrate with ε_r equal to 4.4 and thickness equal to 0.1 mm. The proposed spiral antenna is circular in shape with diameter *'D'* (74 mm). It is mounted on a curved rectangular copper plate of side length *'l x b'* (232 ×150 mm^2) with radius *'Rcurved'* (100 mm). The conducting plate thickness of 3 mm is used for unidirectional radiation with an air gap of *'h'* (9 mm) for better matching, which is shown in Figure 1. The impedance of the antenna input is 160 Ω. The spiral antenna design parameters are optimized in such a way that broadband frequency range could be achieved. The Archimedean spiral is generated by the following mathematical equation –

$$x(t) = (r_0 + a * t) * \cos(t) \quad (1)$$

$$y(t) = (r_0 + a * t) * sin(t) \quad (2)$$

Where, the distance between neighbouring arms denoted by *'a'* (1 mm), and the width of the arm denoted by *'w'* (1.15 mm). The inner radius of the spiral is denoted by the notation *'r_0'* or *'r_{inner}'* (0.48 mm). The outer radius, denoted by *'r_{out}'* (29.85 mm). The spiral antenna emits electromagnetic radiation from a place where the spiral's circumference is one wavelength.

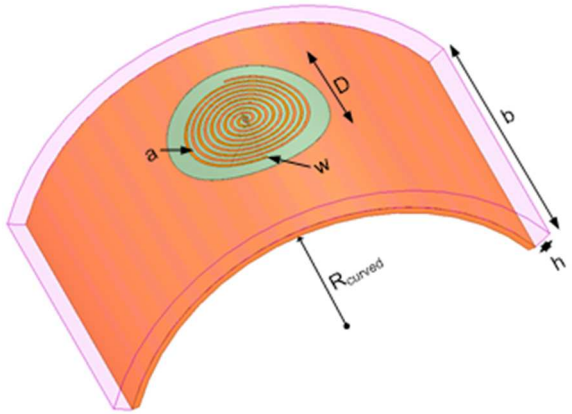

Figure 1. Geometry of the conformal spiral antenna.

This is designated as the spiral's active zone. The currents at complementary or opposing locations on each arm of the spiral are fed 180° out of phase. Thus when the diameter of the spiral is one wavelength, the currents at points on each arm of the spiral that are opposite or complementary come together in phase in the far-field. The arm's width and gap between of each arm can be found from the Equation (3).

$$a = \{(r_{out} - r_{inner})/\, 2 * N\} - w \quad (3)$$

Where, N is the number of turns in the spiral. The theory of operation applies to all spirals, regardless of their shape (circular or square) or type, as long as they are tightly wound (w > 0.25) [8]. The spiral antenna's operation is mainly based on the radiation band theory, which claims that the spiral mostly radiates from annular bands with circumferences that are an integer multiple of a wavelength [9].

2.2 Balun feed mechanism

The balun shown in Figure 2 is an altered planar back-to-back tapered microstrip to parallel strip configuration. The balun structure was built on a FR4 epoxy substrate with $\mathcal{E}_r$ 4.4 and a thickness of 0.8 mm. The proposed balun is made up of two separate parts. One part is the parallel strip that is connected to the antenna. Its impedance is the same as the antenna's input impedance. The other part is a microstrip line with a ground plane that gradually gets narrower until it looks like a parallel strip. The taper does the work of changing the mode and impedance. Balun can be created by solving the following equation:

$$Z(z) = Zo \times e^{(b \times z)} \quad (4)$$

$$b = \frac{1}{l} \times \ln(\frac{Z_L}{Z_0}) \quad (5)$$

Where *'z'* is the place on the length l_b, where l_b is total length of tapper. The microstrip line has an input impedance 50 Ω (Z_0) and output impedance 160 Ω (Z_L). Microstrip output impedance equals parallel strip impedance (Z_L).

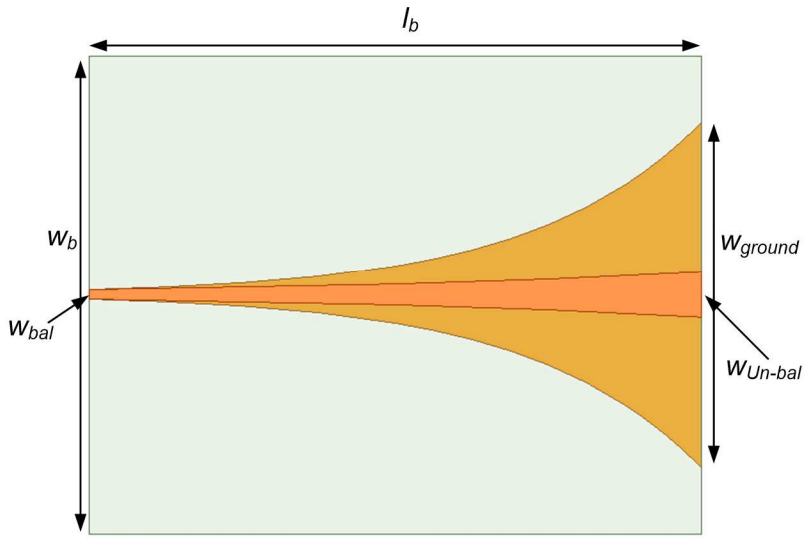

Figure 2. A microstrip-to-parallel-strip balun.

Table 1. The specifications of the Balun for the tapered microstrip to parallel strip connection

Dimensions	Values (Unit in mm)
l_b	20.5
w_b	16
$W_{Un\text{-}bal}$	1.52
W_{bal}	0.32
W_{ground}	11.57

It has been determined that the microstrip line should have an initial width of $W_{\mathbf{Un\text{-}bal}}$ in order to achieve a characteristic impedance of 50 Ω. The characteristic impedance equation is presented in [8], and it is used to calculate the top strip width of the microstrip line. The parameters sweep method, along with the HFSS simulation software, is used to determine the ground plane width, which is denoted by $W_{\mathbf{ground}}$. Repeating this procedure allows for the parallel strip impedance to be brought down to 160 Ω. In [10], an exponential taper equation is provided that can be used to calculate the position *'z'* along the given taper, the total length of the taper denoted by the variable 'l_b'. The two typical impedances (Z_0 and Z_L) that change on the line with position *'z'*.

3. Simulated near-field and far-field characteristics

The conformal antenna design has degradation in the impedance bandwidth due to shape change. So, the analysis has been performed and analyzed. The parametric studies have been performed on the flaring angles (in degrees). The parametric variation in the flaring angle of the curved surface (conformal) for the S-parameter, axial ratio, and realized gain is shown in Figures 3-5.

Here we use Ansoft HFSS EM simulation software to simulate the proposed conformal Archimedean spiral antenna structure. The parametric studies at various flaring angles are depicted in the figures below. As can be seen from the

simulation results, the designed antennas of Reflection coefficient at different flaring angles in intended band (2 GHz to 12 GHZ). These flaring angles are calculated as by using below relation-

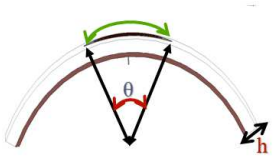

$$\text{Arc length of the spiral} = 2 \times \pi \times R_{curved} \times \frac{\theta}{360} \quad (6)$$

As we have discussed in section 2 that the diameter of the spiral antenna *'D'* (D=74mm) and (Rcurved = 100mm).

Mathematically:

$$74 = 2 \times \pi \times 100 \times \frac{\theta}{360}$$

$$\theta = 42 \text{ degree}$$

All other flaring angles have been calculated in the same way.

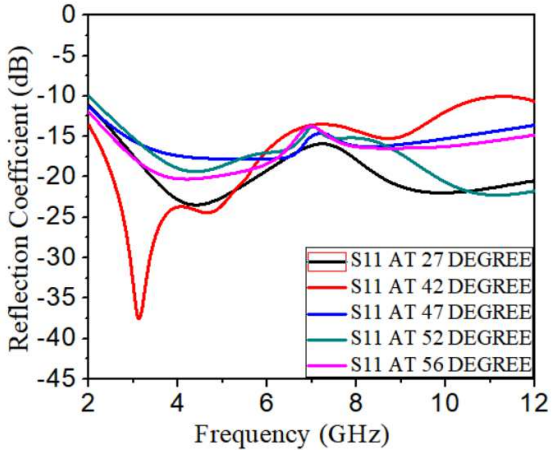

Figure 3. Simulated Reflection Coefficient at different flaring angles.

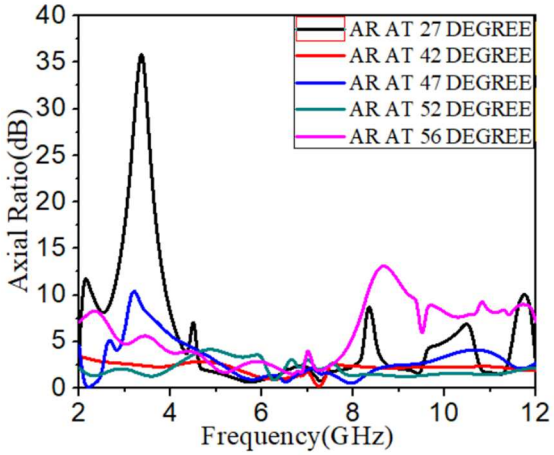

Figure 4. Simulated Axial Ratio plot at different flaring angles.

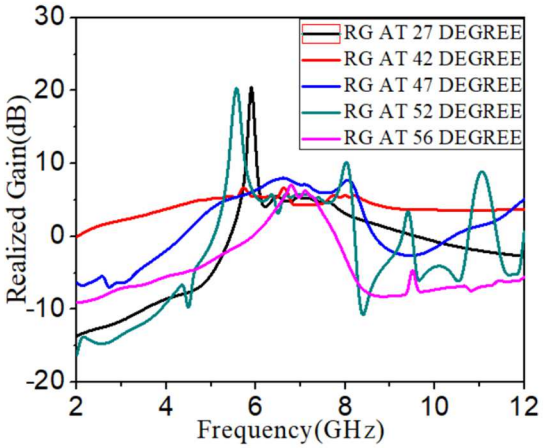

Figure 5. Simulated Realized Gain plot at different flaring angles.

It is noted that in parametric analysis by optimizing the air gap and the depth (R*curved*), the different flaring angles is formed, which helps for achieving better circular polarization. As shown in Figure 4, the axial ratio at 42 degree is the best of all flaring angles. Similarly, Figure 5 shows the realized gain parametric at different flaring angles.

4. Experimental Validation

A prototype of the proposed BSA is fabricated and validated through measurement in an Anechoic chamber, as shown in Figure 6.

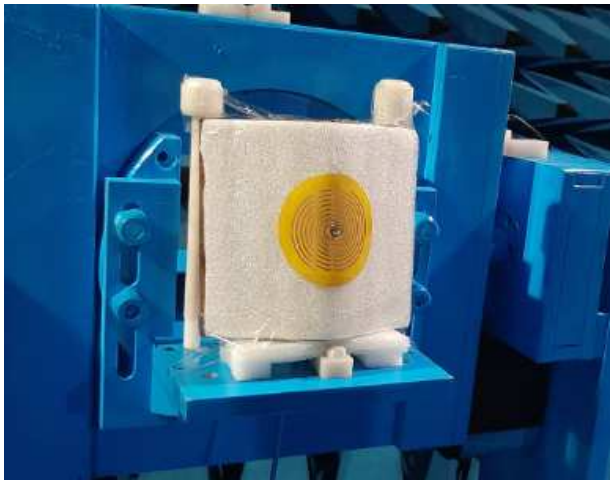

Figure 6. A constructed model of the proposed antenna

Figures 7 and 8 show the proposed antenna's simulated and measured reflection coefficients and axial ratio. Due to manufacturing tolerance, the operating band of CP is observed to be marginally lower than that of impedance bandwidth. The -10dB impedance band spans between 2 and 12 GHz. With a bandwidth of 142%, the axial ratio for CP can be seen to be less than 3 dB. Figure 9, displays the simulated and measured antenna gain results. As a result of degradation on the lower frequency side, the total operating band of the antenna is nearly 140%. Figure.10 shows that when cross polarization is low, good RHCP and LHCP patterns can be made. The simulated and measured outcomes correspond well. It demonstrates its suitability as a candidate for the broadband conformal FI antenna for airborne applications.

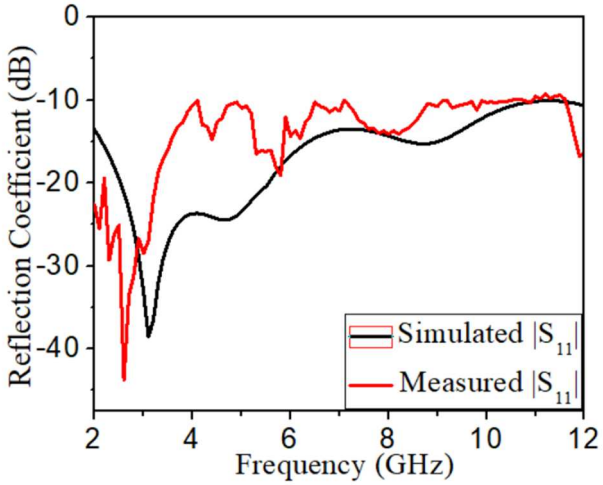

Figure 7. Simulated and measured Reflection Coefficient of the prototype at 42 degree.

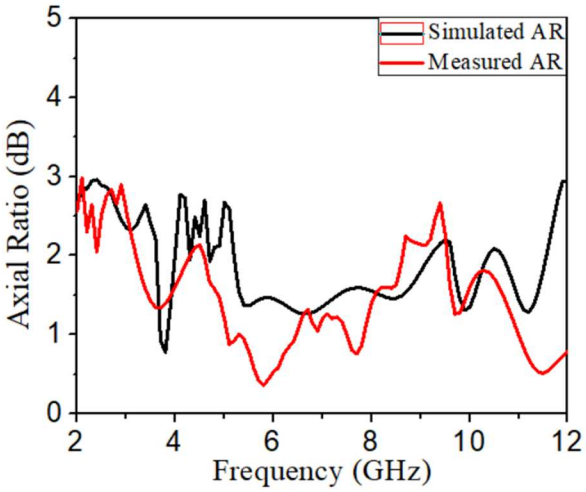

Figure 8. Simulated and measured Axial Ratio of the prototype at the flaring angle of 42 degree.

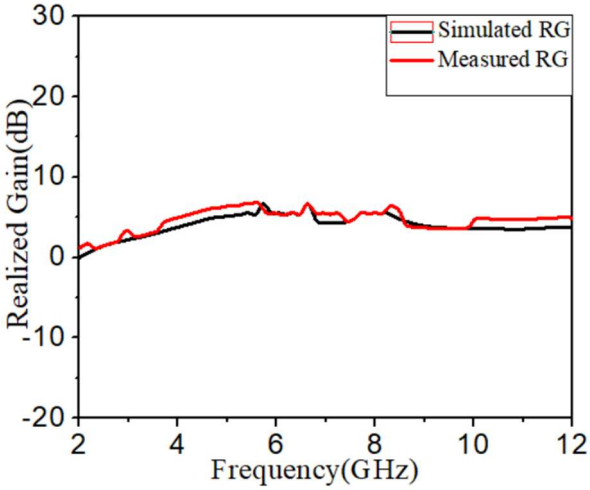

Figure 9. Simulated and Measured Realized Gain plot at the flaring angle of 42 degree.

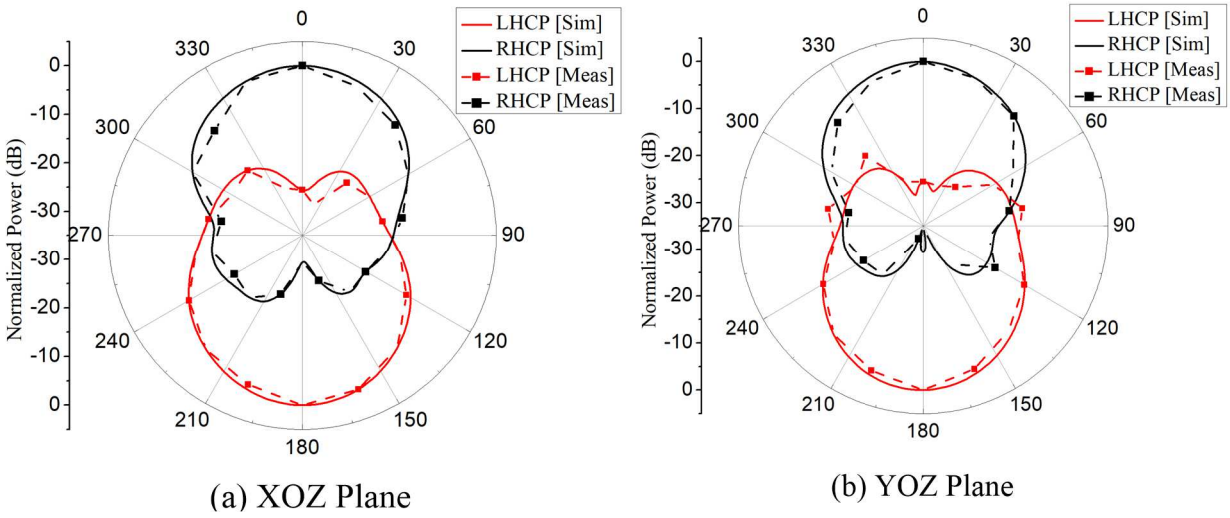

Figure 10. Simulated and Measured LHCP (Left hand CP) and RHCP (Right hand CP) normalized radiation patterns at 6.5 GHz for 42 degree flaring angle (a) XOZ-Plane (b) YOZ-Plane.

5. Conclusion

This paper has presented a conformal broadband spiral antenna suitable for airborne applications. The primary advantages and disadvantages of using conformal antennas have been discovered through this study. In general, conformal antennas are recommended when highly broad-beam radiation patterns are sought. The most significant disadvantage of conformal antennas is their higher manufacturing complexity and cost. The results demonstrate that the conformity has a significant impact on the impedance bandwidth, polarization and gain. Conformal spiral antenna attached to a curved conducting plate with an air gap provides broader beams but with limited back radiation to avoid affecting the polarization characteristics, which makes their integration possible in airborne application. The proposed conformal structure of spiral antenna provides broadside radiation pattern with circular polarization in overall bandwidth. The experimental verification of the proposed antenna has an overall bandwidth ($|S_{11}| < -10$ dB, AR < 3 dB) of 140 % with a maximum of 5.3 dBic realized gain.

6. References

1. C. Sairam, T. Khumanthem, S. Ahirwar and S. Singh, "Broadband blade antenna for airborne applications," 2011 Annual IEEE India Conference, 2011, pp. 1-4, doi: 10.1109/INDCON.2011.6139414
2. W. Zhao, L. Li, E. Li and K. Xiao, "Analysis of Radiation Characteristics of Conformal Microstrip Arrays Using Adaptive Integral Method," in IEEE Transactions on Antennas and Propagation, vol. **60**, no. 2, pp. 1176-1181, Feb. 2012, doi: 10.1109/TAP.2011.2173135
3. Conformal Antenna Array Design Handbook, Alexandria, VA:NTIS, 1981
4. J. Meiguni and D. Pommerenke, "Theory and Experiment of UWB Archimedean Conformal Spiral Antennas," in IEEE Transactions on Antennas and Propagation, vol. **67**, no. 10, pp. 6371-6377, Oct. 2019, doi: 10.1109/TAP.2019.2925183
5. H. Nakano, S. Sasaki, H. Oyanagi, and J. Yamauchi, "Cavity-backed Archimedean spiral antenna with strip absorber," IET Microw., Antennas Propag., vol. **2**, no. 7, pp. 725–730, Oct. 2008, doi: 10.1049/iet-map:20080022
6. J. Dyson, "The characteristics and design of the conical log-spiral antenna," in IEEE Transactions on Antennas and Propagation, vol. **13**, no. 4, pp. 488-499, July 1965, doi: 10.1109/TAP.1965.1138471.
7. P. E. Mayes, "Frequency-independent antennas and broad-band derivatives thereof," in Proceedings of the IEEE, vol. **80**, no. 1, pp. 103-112, Jan. 1992, doi: 10.1109/5.119570

8. María, “Analysis of Conformal Antennas for Avionics Applications”, Master’s Thesis, wireless comm., Chalmers University of Technology Gothenburg, Sweden, 2007, doi: elib.dlr.de/47573
9. S. P. Gao, B. Wang, H. Zhao, W. -J. Zhao and C. E. Png, "Installed Radiation Pattern of Patch Antennas: Prediction based on a novel equivalent model.," in *IEEE Antennas and Propagation Magazine*, vol. **57**, no. 3, pp. 81-94, June 2015, doi: 10.1109/MAP.2015.2437275.
10. M. Kobayashi and N. Sawada, "Analysis and synthesis of tapered microstrip transmission lines," in IEEE Transactions on Microwave Theory and Techniques, vol. **40**, no. 8, pp. 1642-1646, Aug. 1992, doi:10.1109/22.149542